Biomedical Signal Processing and Control 89 (2024) 105815

Contents lists available at ScienceDirect

Biomedical Signal Processing and Control

journal homepage: www.elsevier.com/locate/bspc

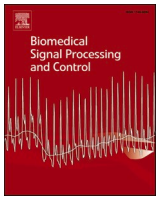

3D convolutional neural network for schizophrenia detection using as EEG-based functional brain network

Mingkan Shen [a,*], Peng Wen [a], Bo Song [a], Yan Li [b]

[a] School of Engineering, University of Southern Queensland, Toowoomba, Australia
[b] School of Mathematics, Physics and Computing, University of Southern Queensland, Toowoomba, Australia

ARTICLE INFO

Keywords:
ScZ
EEG
Multivariate autoregressive model
Coherence
3D-CNN
Brain network analysis

ABSTRACT

Schizophrenia (ScZ) is a chronic mental disorder affecting the function of the brain, which causes emotional, social, and cognitive problems. This paper explored the functional brain network and deep learning methods to detect ScZ using electroencephalogram (EEG) signals. Functional brain network analysis was proposed and implemented using a multivariate autoregressive model and coherence connectivity algorithm. The three machine learning techniques and 3D-convolutional neural network (CNN) models were applied to classify the ScZ patients and health control subjects, and then the public LMSU database was utilized to assess the performance. The proposed 3D-CNN method achieved the performance of a 98.47 ± 1.47 % in accuracy, 99.26 ± 1.07 % in sensitivity, and 97.23 ± 3.76 % in specificity. Moreover, in addition to the default mode network region, the temporal and posterior temporal lobes of both right and left hemispheres were found as the significant difference areas in ScZ brain network analysis.

1. Introduction

Schizophrenia (ScZ) is a mental neuropsychiatric disorder of the brain, which affects emotional behaviours, persistent delusions, and cognitive deficit symptoms [1–3]. Regarding to the report of World Health Organization in 2022, approximately 24 million people suffered from ScZ disease [4]. In clinical detection, electroencephalogram (EEG) is an auxiliary approach to detect brain's electronic signal, which can provide high accuracy detection without any physical intrusion [5]. Compared with other two popular brain detection techniques, functional magnetic resonance imaging (f-MRI) and magnetoencephalography (MEG), EEG presents two prominent advantages: it demands less extensive training for operators, making it more accessible for medical professionals, and it involves significantly lower equipment costs, making it a cost-effective option for brain monitoring and research [6,7].

Majority of researchers, in recent years, detected the ScZ diseases through functional brain network analysis using f-MRI data because the f-MRI technique can directly solve the space resolution problem [8–10]. Long, Q, et al. utilized independent vector analysis to extract common subspace components from fMRI data in individuals with ScZ and health control (HC) participants [8]. They found significant differences in functional brain networks between the two groups. The results of their study contribute to our understanding of the neural mechanisms underlying ScZ and provide insights into the potential biomarkers or targets for diagnosis and treatment. Fu, Z et al. applied a brain activity-connectivity algorithm to fMRI data from individuals diagnosed with ScZ [9]. This algorithm involved estimating brain activity fluctuations and assessing connectivity patterns between different brain regions. By covarying the brain activity with connectivity measures, the researchers investigated how changes in brain activity related to fluctuations in network efficiency. Zhang, G et al. applied the Joint directed acyclic graph estimation model to detect abnormal fMRI connectivity in ScZ [10]. Their findings revealed decreased functional integration, disrupted hub structures, and characteristic edges in ScZ subjects. These results contribute to the understanding of the neural underpinnings of ScZ and provide insights into the specific connectivity abnormalities associated with the disorder. Inspired by the deep understanding of ScZ diseases through functional brain network analysis in f-MRI data, the functional brain network analysis is explored into EEG signal in this study.

The default mode network (DMN) has been found to exhibit significant differences in resting-state brain activity between individuals with ScZ and HC subjects [11]. The DMN is a network of brain regions that

* Corresponding author.
E-mail address: u1095095@umail.usq.edu.au (M. Shen).

https://doi.org/10.1016/j.bspc.2023.105815
Received 17 May 2023; Received in revised form 23 October 2023; Accepted 29 November 2023
Available online 6 December 2023

are consistently active during rest and are involved in self-referential thinking, introspection, and mind-wandering. The DMN consists of several key areas, including the mesial prefrontal cortex (MPC), the lateral posterior cortex (LPC), and the posterior cingulate cortex/precuneus (PCC) [11]. Zhang, S et al. applied the DMN region as a node of f-MRI data to detect abnormal ScZ connectivity [12]. F-MRI DMN functional connectivity analysis was also utilized via Fan. J et al to detect ScZ and obsessive–compulsive disorder [13]. However, the study conducted by Phang et al. focused on the functional brain network analysis of ScZ [14]. They employed whole brain connectivity analysis, which involves investigating the connections and interactions among all brain regions, rather than focusing solely on local brain networks. Based on the information provided, the study highlights the importance of considering the entire brain's functional connectivity, including regions within the DMN, to gain a more complete understanding of the abnormal brain activity in ScZ.

In EEG analysis, traditional signal processing and machine learning, as well as deep learning models, have been widely employed in classifying EEG ScZ signals. Baygin, M et al. proposed collatz pattern technique and K-nearest neighbour (k-NN) classifier to detect EEG ScZ patients and achieved 99.47 % and 93.58 % in accuracy using two public ScZ databases [15]. Akbari et al. calculated ScZ features through phase space dynamic features and employed the k-NN model for classification [16]. Their research reported an accuracy of 94.80 %, sensitivity of 94.30 %, and specificity of 95.20 %. Lillo et al. utilized a convolutional neural network (CNN) to identify ScZ diseases and achieved a success rate of 93 % in accuracy [17]. They also highlighted the ability of their study to achieve computer-assisted diagnosis in just 3 min. Supakar et al. proposed a deep learning model that combines recurrent neural network (RNN) and long short-term memory (LSTM) network to detect ScZ using the Lomonosov Moscow State University (LMSU) dataset [18]. They achieved an accuracy of 98 % in their experiment. Sairamya et al. employed the discrete wavelet transform (DWT) and relaxed local neighbour difference pattern (RLNDiP) technique to detect ScZ in the LMSU database [19]. Their approach yielded a maximum accuracy of 100 % in their experiment. Hassan et al. applied CNN to extract ScZ signal features and classified the features using the logistic regression method [20]. They obtained accuracies of 90 % and 98 % on subject-based and non-subject-based testing, respectively. Gosala et al. utilized the wavelet scattering transform (WST) as a signal processing method to detect ScZ EEG signals [21]. They reported accuracy rates of 97.98 %, sensitivity of 98.2 %, specificity of 97.72 %, and a Kappa score of 95.94 % in SVM classification.

The functional brain network is also applied to provide biomarkers of the ScZ diseases. Wang, J et al. investigated the left frontal-parietal/temporal networks and found biomarkers of auditory verbal hallucinations (AVH) in ScZ diseases through phase locking value (PLV) connectivity algorithm. They also achieved a classification result of 80.95 % accuracy in AVH patients and non-AVH patients [22]. Prieto-Alcantara et al. explored neurophysiological differences in different cognitive states between ScZ patients and HC subjects using the EEG coherence connectivity method [23]. Their study provided evidence of these differences and highlighted the potential of functional connectivity analysis in understanding ScZ. In our previous work, dynamic functional connectivity analysis using the cross mutual information (CMI) algorithm with a 3D CNN was applied to identify ScZ EEG signals [24]. The results showed an accuracy of 97.74 ± 1.15 %, sensitivity of 96.91 ± 2.76 %, and specificity of 98.53 ± 1.97 %. Furthermore, the fuzzy localization of ScZ diseases was investigated in this study as well.

The multivariate auto-regressive model (MVAR) coherence functional brain network method with 3D-CNN model is applied to detect the EEG ScZ signal in this Study. The MVAR coherence method was utilized to estimate the connectivity between different brain regions based on EEG data. This method allows for the extraction of frequency domain features, enabling the identification of abnormal connectivity areas associated with ScZ. After that, the 3D-CNN model was designed to classify functional brain network features between ScZ patients and HC subjects. This model leverages the extracted features from the MVAR coherence brain network to differentiate between the two groups. The sliding window technique was employed to capture the dynamic changes in ScZ by considering the time-varying nature of the functional brain network. This technique allows for the analysis of EEG signals in small overlapping windows, considering temporal variations and improving the accuracy of the experiment. Moreover, the study analysed different brain rhythms to reduce computational costs. It found that the α band (8–12 Hz) demonstrated the best performance in testing data. This suggests that focusing on the α band frequency range yields meaningful results in the context of ScZ analysis. Furthermore, the study performed statistical analysis on the whole brain connectivity to verify abnormal connectivity areas. Specifically, abnormal connectivity areas were identified in the DMN region, as well as the temporal lobe and posterior temporal lobe of both hemispheres. All the experiments are simulated in MATLAB 2021b software on a Dell workstation with an NVIDIA 3080TI GPU.

In this paper, Section 1 introduces the research background and the related works in recent years. The objectives this study is also included in this section. Section 2 describes the proposed methodology, which includes the data pre-processing, signal processing method, functional brain network analysis and classification models. The dataset details are also report in this section. The results and comparison of the experiment are listed in Section 3. In Section 4, statistical analysis of whole brain connectivity, dynamic analysis and the comparison with previous work are discussed while the conclusion is made in Section 5.

2. Methodology

Five main procedures in ScZ detection based on the EEG signal are briefly summarized in Fig. 1. There are two pre-processing steps, including denoised the EEG raw data and the sliding window size selection, to remove the artifacts and extend dynamic research. MVAR model is introduced to transform data from the time domain into the frequency domain, which can provide more spectrum information in different brain rhythms. To extract the brain graph features, the coherence algorithm is applied to construct the functional brain network. Machine learning models and 3D-CNN are used to classify the ScZ subjects and HC subjects using their brain graph features. Finally, three parameters are proposed to evaluate the designed method in this study.

2.1. Datasets and pre-processing

In the evaluation of the proposed methodology for EEG ScZ detection, the researchers utilized a publicly available database called LMSU [25,26]. This database consisted of EEG recordings from a total of 84 subjects, including 45 individuals diagnosed with ScZ and 39 HC subjects. The LMSU dataset provided EEG signals collected from 16 channels, namely F7, F3, F4, F8, T3, C3, Cz, C4, T4, T5, P3, Pz, P4, T6, O1, and O2. The sampling rate of the EEG signals in this dataset was 128 Hz.

By using a sliding window with a 30-second size and a 1-second overlap, the study considered short-term variations in the EEG signal, which can provide insights into the dynamic changes in brain activity associated with ScZ. The choice of these parameters indicates that the proposed methodology can potentially be applied in real-time applications, as it allows for continuous monitoring and analysis of the EEG signal. To prepare the EEG data for analysis, a 6th-order Butterworth zero-phase filter was applied to the raw data. This filter had a passband frequency range of 1–50 Hz. The purpose of this filtering step was to denoise the EEG signals and remove any artifacts that may have been present.

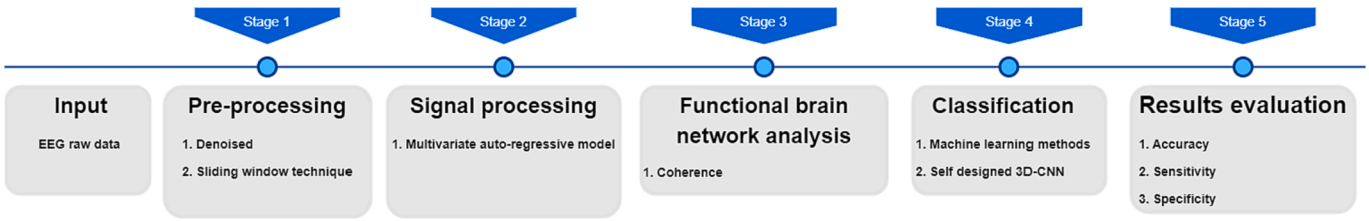

Fig. 1. The progress of ScZ automatic identification.

2.2. Multivariate auto-regressive model

The MVAR model is used to analyse multivariate time series data, such as EEG signals, by representing the relationships between variables, which is applied to convert the denoised EEG data into frequency domain features within the α band (8–12 Hz). The algorithm of MVAR model is illustrated in formula (1).

$$X(n) = \sum_{k=1}^{p} A(k) \times X(n-k) + W(n) \tag{1}$$

where *A(k)* are M × M coefficient matrix which calculates the linear interaction in lag k from $x_j(n-k)$ to $x_i(n), (i,j = 1,\ldots,M)$ of MVAR model. *W(n)* represents a column vector of model errors or innovations in the form of Gaussian noise, characterized by a covariance matrix Σ. To calculate the coefficient matrix *A(k)* and covariance matrix Σ, the Yule-Walker equation is used to describe the relationship between two matrices [27]. p is the order of the MVAR model and calculated via the Akaike Information Criterion (AIC) algorithm. The AIC can select the order number fitting effect of the model and avoid the phenomenon of overfitting when the p is too large. The formula of AIC is shown in equation (2).

$$AIC(p) = -\ln(\widehat{l}) + 2k \tag{2}$$

In equation (2), k is the total parameters used for model fitting and $\ln(\widehat{l})$ is the maximum likelihood estimations of log likelihood. To convert the EEG data into frequency domain spectrum, the Fourier transform is employed. The transfer matrix of MVAR model *H(f)*, and cross-spectrum matrix *S(f)* are estimated in equation (3) and (4).

$$H(f) = \left(\sum_{k=0}^{p} -A_k e^{-jk2\pi f} \right)^{-1} \tag{3}$$

$$S(f) = H(f) \sum \left(H^H(f) \right) \tag{4}$$

where $H(f)$ is the spectral matrix at frequency '*f*', $H^H(f)$ is the conjugate transpose of $H(f)$,Σ is the noise covariance matrix. A_k is the parameter of M × M coefficient matrix, '*p*' is the model order and '*j*' represents the imaginary unit.

2.3. Functional brain network analysis

The coherence connectivity based MVAR model is applied to construct the functional brain network in the corresponding frequency domain. The algorithm of magnitude-squared coherence between two different channels is shown in equation (5):

$$coh_{xy}(f) = \left| \frac{S_{xy}(f)}{\sqrt{S_{xx}(f) S_{yy}(f)}} \right|^2 \tag{5}$$

where the $S_{xx}(f)\mathrm{H}(\mathrm{F_i})$ is the power spectrum density of x, the $S_{yy}(f)\mathrm{H}(\mathrm{F_i})$ is the power spectrum density of y, and $S_{xy}(f)\mathrm{H}(\mathrm{F_i})$ is the cross-spectral power spectrum density between x and y.

In the described experiment, to extract more information from the MVAR coherence connectivity matrix, the functional brain network is computed for each frequency range within the α band. Specifically, the frequency ranges of 8–9 Hz, 9–10 Hz, 10–11 Hz, and 11–12 Hz are considered. Since the experiment involves EEG data from 16 channels, the resulting matrix has dimensions of 16 × 16. For instance, the 4-level functional brain network of a subject '*022w*' in ScZ case is illustrated in Fig. 2.

2.4. Classification

After the features of the functional brain network have been extracted from the EEG raw signal, the next task is to classify the features between ScZ patients and HC subjects through machine learning and deep learning methods. In this study, three machine learning methods include SVM, k-NN and decision tree (DT) models, and the proposed 3D-CNN were used to classify the testing data.

2.4.1. Leaving one group out training method

By using the leaving one group out method, the experiment aims to assess the generalizability and performance of the model on unseen data. It helps to ensure that the model is not biased or overfitted to a specific group of subjects. Therefore, five models have been established in this study. The details of the 5-group dataset are summarized in Table 1.

2.4.2. Machine learning methods

The Classification Learner Toolbox in MATLAB 2021b is applied in this part. In training progress, 80 % of the data is used for training, and the remaining 20 % is set aside for validation. The training set is used to train the models, while the validation set is used to evaluate their performance and tune any hyperparameters. The validation accuracy is listed in the Table 2.

In the functional brain network, the matrix is symmetrical and the coherence value between the same node equals 0. To reduce the computational cost, about (16 × 16–16) / 2 × 4 = 480 values of the 4-layer functional brain network matrix are selected as input.

2.4.3. Deep learning method

In functional brain network analysis, the brain is regarded as a large-scale network, which is also known as the brain graph that consists of the nodes and edges. The nodes here are the EEG channels, and the edges are the brain connectivity. CNN is an advanced deep learning method that has been successfully applied in photograph classifications, such as Google-net CNN, VGG-net CNN, and Alex-net CNN. Therefore, the 3D-CNN is designed and employed to classify the brain graph data in this study. The architecture of the 10-layer 3D-CNN is shown in the Fig. 3.

The designed 3D-CNN model in the experiment consists of four convolution layers, three ReLU layers, one max pooling layer, and one fully connected layer. The architecture aims to classify subjects with ScZ and HC subjects. To address overfitting, batch normalization is applied in the four convolution layers. Batch normalization helps stabilize and normalize the activations within each mini batch during training, reducing the likelihood of overfitting. The first convolution layer has a kernel size of 3 × 3 × 3 and 64 channels. After this layer, a max pooling layer is employed to reduce the dimensions of the 3D-image input into

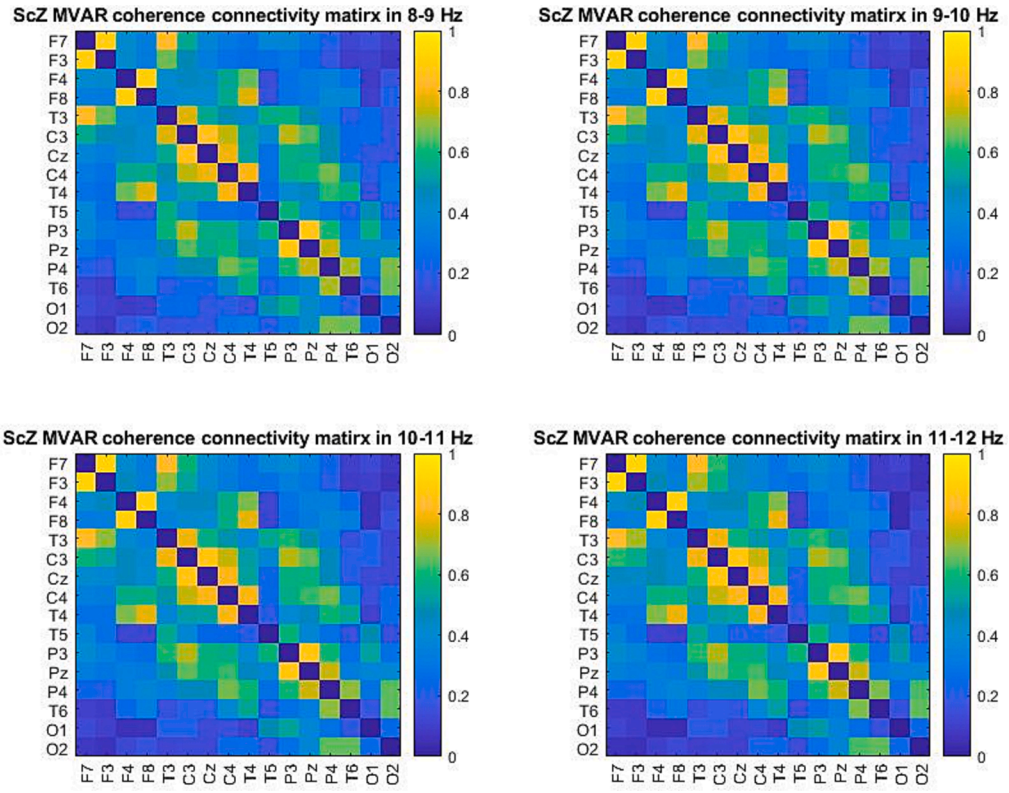

Fig. 2. Functional brain network of subject *'022w'* in ScZ case.

Table 1
Five-group data for classification.

	ScZ dataset	HC dataset
Group A	022w, 32w, 219w, 221w, 387-02w, 387-03w, 510-1w, 515w, 642w	s10w, s12w, s43w, s47w, s78w, s85w, s158w, s174w
Group B	33w, 088w, 249w, 276w, 401w, 423w, 517w, 683w, 719w	s18w, s20w, s50w, s94w, s163w, s164w, s176w, s177w
Group C	103w, 113w, 307w, 312w, 429w, 454-1w, 540w, 548w, r229w	s26w, s53w, s55w, s152w, s153w, s165w. s167w, s178w
Group D	155w, 156w, 314w, 485w, 508w, 573w, 575w, r416w, s083w	s27w, s31w, s59w, s60w, s154w, s169w, s170w, s179w
Group E	192w, s084-1w, 342w, 382w, 509w, s351w, 585w, 586w, s425w	s42w, s72w, s155w, s157w, s173w, s182w, s196w

Table 2
The Validation accuracy of SVM, k-NN and DT.

	Test group	SVM	KNN	DT
Validation accuracy (%)	Group A	99.52	100.00	98.21
	Group B	100.00	100.00	97.98
	Group C	100.00	100.00	99.41
	Group D	99.08	100.00	98.33
	Group E	99.73	100.00	99.03
	Mean ± Std	99.67 ± 0.38	100.00 ± 0.00	98.59 ± 0.60

2D-image data. The subsequent three convolution layers all have a kernel size of $3 \times 3 \times 1$ and 64 channels. The purpose of these layers is to capture relevant features from the input data. A max pooling layer with a size of $2 \times 2 \times 2$ and a stride of $2 \times 2 \times 2$ is used to down sample the feature maps and reduce the computational cost during training. ReLU layers follow each convolution layer. The ReLU activation function introduces non-linearity to the model by setting negative values to zero, allowing the network to learn complex patterns and improve its representational power. Since the experiment focuses on classifying ScZ and HC subjects, the fully connected layer is designed for two-class classification. This layer aggregates the learned features and performs classification based on the extracted information. The last layer of the architecture is a Softmax classifier, which provides the prediction results of the proposed method. The Softmax function assigns probabilities to each class, indicating the model's confidence in its predictions. The details of the input size and output size of each layer are summarized in Table 3.

The same validation method with 50 iterations validation frequency is used in the designed 3D-CNN model and achieved 100 % validation accuracy using the leaving one group out training method. The optimizer of the proposed deep learning model in MATLAB 2021b is shown in Fig. 4.

3. Results and comparison

In the evaluation of the proposed method for EEG ScZ detection using the LMSU database, accuracy, sensitivity, and specificity are calculated as performance metrics. Accuracy represents the proportion of correctly classified samples (both true positives and true negatives) out of the total number of samples. Higher accuracy values indicate better performance in classifying ScZ and HC subjects. The formula of accuracy is described in equation (6).

$$Acc = \frac{TP + TN}{TP + TN + FP + FN} \tag{6}$$

where *'TP'*, *'TN'*, *'FP'*, *'FN'* correspond to the true positive, true negative, false positive and false negative.

Sensitivity, also known as true positive rate or recall, measures the proportion of ScZ subjects that are correctly identified as positive by the classification model. It indicates the ability of the method to correctly detect ScZ cases. Higher sensitivity values indicate a lower rate of false negatives, suggesting a better ability to identify true positive ScZ subjects. The algorithm of sensitivity is shown in equation (7).

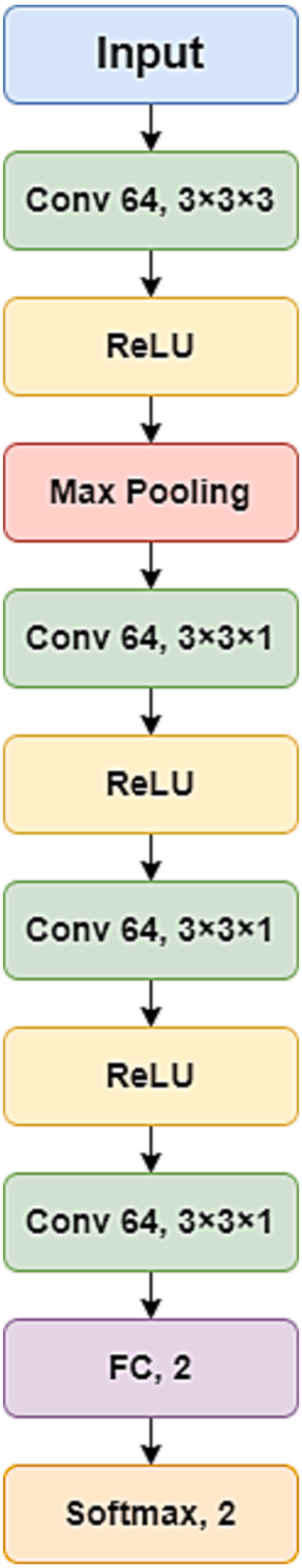

Fig. 3. 10-layer 3D-CNN architecture, '*Conv*' is the convolution layer and '*FC*' is the fully connected layer.

Table 3
The details of deep learning method architecture.

Layer Level	Input Size	Output Size	hyperparameters
–	16 × 16 × 4 × 1		
Level 1 (Conv)	16 × 16 × 4 × 1	14 × 14 × 2 × 64	Kernel size: 3 × 3 × 3 Stride: 1 × 1 × 1 Channel: 64
Level 2 (ReLU)	14 × 14 × 2 × 64	14 × 14 × 2 × 64	
Level 3 (Max Pooling)	14 × 14 × 2 × 64	7 × 7 × 1 × 64	Pooling Size: 2 × 2 × 2 Stride: 2 × 2 × 2
Level 4 (Conv)	7 × 7 × 1 × 64	5 × 5 × 1 × 64	Kernel size: 3 × 3 × 1 Stride: 1 × 1 × 1 Channel: 64
Level 5 (ReLU)	5 × 5 × 1 × 64	5 × 5 × 1 × 64	
Level 6 (Conv)	5 × 5 × 1 × 64	3 × 3 × 1 × 64	Kernel size: 3 × 3 × 1 Stride: 1 × 1 × 1 Channel: 64
Level 7 (ReLU)	3 × 3 × 1 × 64	3 × 3 × 1 × 64	
Level 8 (Conv)	3 × 3 × 1 × 64	1 × 1 × 1 × 64	Kernel size: 3 × 3 × 1 Stride: 1 × 1 × 1 Channel: 64
Level 9 (FC)	1 × 1 × 1 × 64	1 × 1 × 1 × 2	
Level 10 (Softmax)	1 × 1 × 1 × 2		

* '*Conv*' is the convolution layer and '*FC*' the fully connected layer.

$$Sen = \frac{TP}{TP + FN} \tag{7}$$

Specificity measures the proportion of HC subjects that are correctly identified as negative by the classification model. It represents the ability of the method to correctly identify HC cases. Higher specificity values indicate a lower rate of false positives, indicating a better ability to correctly identify true negative HC subjects.

$$Spe = \frac{TN}{TN + FP} \tag{8}$$

3.1. Results of the proposed method

Three machine learning methods, SVM, k-NN and DT, and the proposed 3D-CNN are used to detect EEG ScZ functional brain network. From Table 4, the proposed 3D-CNN has achieved the best performance in this study, which reports the results of 98.47 ± 1.47 % accuracy, 99.26 ± 1.07 % sensitivity, and 97.23 ± 3.76 % specificity of testing data.

According to Table IV, these three machine learning models achieve very high validation result, but they could not overcome the robustness problem. Furthermore, the standard deviation of the proposed method is significantly smaller than the machine learning methods, which implies that every subject can be detected stably through the 3D-CNN model. It also indicates that the proposed 3D-CNN model can be used in the clinical applications.

3.2. Comparison with different complex brain network methods

Based on the MVAR model, five other connectivity algorithms are used to evaluate the proposed method, which includes the directed coherence (DC), directed transform function (DTF), PDC, generalized partial directed coherence (GPDC) and partial coherence (PCO). The details of the comparison are shown in Table 5.

The effective connectivity methods, including DC, DTF, PDC, GPDC algorithm, consider the directionality of brain connectivity, which can determine the causality information between the connectivity. However, it cannot obtain high-accuracy detection results in this study as shown in Table 5.

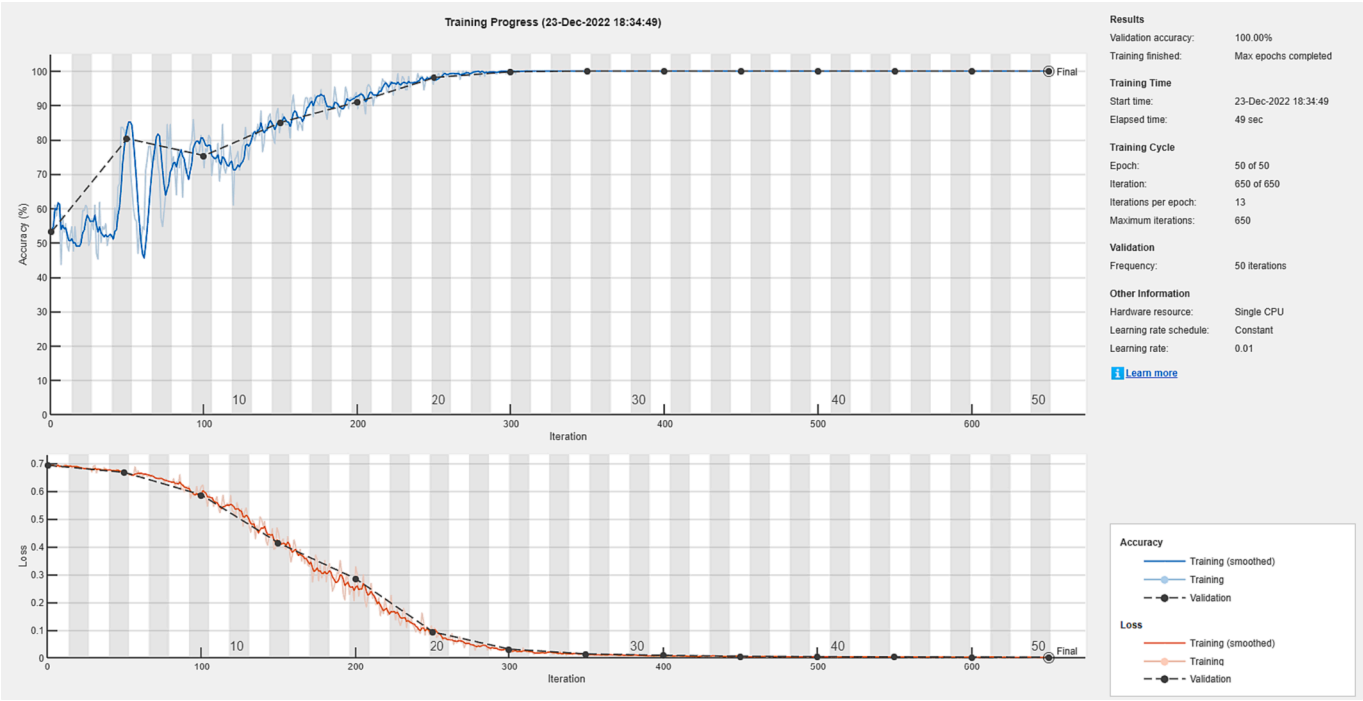

Fig. 4. The optimizer of self-designed 3D-CNN model of testing group A.

Table 4
The test results for SVM, k-NN, DT and 3D-CNN model.

Results	Test group	SVM	k-NN	DT	3D-CNN
Accuracy (%)	Group A	89.92	77.22	74.19	98.59
	Group B	84.48	79.23	79.64	98.19
	Group C	79.81	74.80	79.44	96.17
	Group D	89.52	74.60	76.01	100.00
	Group E	84.48	80.44	77.22	99.40
	Mean ±	85.64 ±	77.26 ±	77.30 ±	**98.47 ±**
	Std	4.18	2.60	2.31	**1.47**
Sensitivity (%)	Group A	86.46	73.21	90.83	97.67
	Group B	76.72	79.52	76.42	100.00
	Group C	76.86	70.54	83.63	100.00
	Group D	86.34	71.16	84.03	100.00
	Group E	81.53	74.59	82.91	98.64
	Mean ±	81.58 ±	73.80 ±	83.56 ±	**99.26 ±**
	Std	4.81	3.58	5.11	**1.07**
Specificity (%)	Group A	91.24	75.58	45.62	99.07
	Group B	92.63	73.57	78.83	95.85
	Group C	80.52	72.81	65.90	91.24
	Group D	90.32	70.51	55.76	100.00
	Group E	83.41	83.87	60.37	100.00
	Mean ±	87.62 ±	75.27 ±	61.30 ±	**97.23 ±**
	Std	5.33	5.14	12.31	**3.76**

Table 5
The comparison between different connectivity methods.

Connectivity method	Accuracy (%)	Sensitivity (%)	Specificity (%)
DC	74.44 ± 6.78	77.24 ± 12.90	62.67 ± 18.17
DTF	72.06 ± 4.31	71.30 ± 6.87	61.11 ± 5.41
PDC	79.32 ± 6.12	85.37 ± 3.19	63.96 ± 17.44
GPDC	78.87 ± 5.40	90.29 ± 12.93	62.03 ± 23.35
PCO	81.29 ± 10.39	77.63 ± 11.86	80.55 ± 11.99
Proposed method	**98.47 ± 1.47**	**99.26 ± 1.07**	**97.23 ± 3.76**

3.3. Comparison with different frequency bands

In EEG studies focused on detecting ScZ and studying the neural markers of disorders, researchers typically investigate a range of brain rhythms, with a particular emphasis on deviations or abnormalities from normal patterns. Frequency band selection in EEG experiments related to ScZ is a critical step that allows researchers to focus their analyses on specific aspects of neural activity that are most relevant to the disorder. This targeted approach helps uncover meaningful insights and potential biomarkers associated with ScZ, facilitating both research and clinical applications. The frequency band selection is performed to optimize computing costs while maintaining the effectiveness of EEG ScZ identification in this experiment. The MVAR coherence is constructed in different frequency bands, namely δ band (0–4 Hz), θ band (4–8 Hz), α band (8–12 Hz), β-1 band (12–16 Hz), β-2 band (16–20 Hz), β-3 band (20–24 Hz), and β-4 band (24–28 Hz). The purpose is to identify the brain rhythms within these frequency bands that yield the best results in EEG ScZ identification. The results of this analysis are summarized in Table 6, which provides information on the performance metrics (such as accuracy, sensitivity, and specificity) achieved in each frequency band.

According to Table 6, the α band brain rhythm has been verified as the best frequency band to detect the ScZ from EEG signal. The previous work stated that alterations in α rhythms have been reported in ScZ, potentially related to disruptions in sensory gating and attention processes [28]. This comparison also proves that α rhythms, particularly in the resting state with eyes closed, can provide insights into the

Table 6
The comparison between different frequency band.

Frequency band	Accuracy (%)	Sensitivity (%)	Specificity (%)
δ band (0–4 Hz)	85.04 ± 5.30	80.42 ± 6.59	87.37 ± 5.76
θ band (4–8 Hz)	90.20 ± 4.23	85.85 ± 2.60	92.81 ± 8.56
α band (8–12 Hz)	**98.47 ± 1.47**	**99.26 ± 1.07**	**97.23 ± 3.76**
β-1 band (12–16 Hz)	92.39 ± 4.49	91.78 ± 5.46	90.78 ± 5.21
β-2 band (16–20 Hz)	92.42 ± 5.60	92.20 ± 7.49	90.60 ± 5.98
β-3 band (20–24 Hz)	92.82 ± 5.34	92.58 ± 5.92	90.97 ± 8.71
β-4 band (24–28 Hz)	91.17 ± 7.05	87.36 ± 8.76	93.73 ± 7.41

functional connectivity and synchronization of brain regions.

4. Discussion

4.1. Statistical analysis of MVAR coherence connectivity

In functional brain network analysis, different brain regions correspond to different functions. Through the statistical analysis of brain connectivity value, the biomarker of abnormal connectivity between the ScZ patients and HC subjects can be found. DMN region is the most significant part of the brain, which is related to the function of sensory, motor executive control and visual components [29]. There are three brain regions in DMN, including LPC, MPC and PCC [11]. In EEG analysis, Brodmann areas (BA) are applied to correspond to the DMN region with the EEG electrodes and the details shown in Table 7 [30,31].

Based on the derived mean value and standard deviation of the whole brain connectivity of the functional brain network, the abnormal connectivities with the major difference mean value (≥0.10) between ScZ subjects and HC subjects are listed in Table 8.

From the statistical analysis results of Table VIII, not only the connectivity of DMN regions but also the connectivity of T4 - T6 and T3 - T5 are the biomarkers of the ScZ disease, which corresponds to the temporal lobe and posterior temporal lobe area in both right and left side. It also indicates that the whole brain connectivity analysis of the functional brain network is necessary.

4.2. Dynamic analysis

In dynamic connectivity analysis of EEG signal for ScZ detection, the selection of an appropriate sliding window size is critical for capturing the temporal dynamics of functional connectivity patterns in brain. Dynamic connectivity analysis aims to examine how the strength and patterns of functional connections between brain regions change over time. Considering the temporal characteristics of ScZ-related neural phenomena. ScZ is associated with both rapid and slower changes in brain activities. Larger window sizes tend to smooth out rapid changes and variations in EEG signal, potentially leading to a loss of important temporal information. This can make it challenging to cluster and analyse the dynamic patterns associated with ScZ accurately. On the other hand, the selection of a window too small can lead to decreased accuracy. Smaller window sizes might not capture sufficient information about the temporal dynamics of ScZ, and the analysis may be affected by noise or random fluctuations within shorter time intervals. This can result in decreased sensitivity and specificity of the method. As a result, the sliding window size of 3-second, 5-second. 10-second, 30-second and 40-second are evaluated with the proposed method, and the results are shown in Table 9.

The 30-second size can achieve the best performance in this study based on the above table. A smaller sliding window size makes it hard to capture the slower changes in brain function of ScZ diseases, and the maximum 40-second size segment creates a loss of temporal precision.

4.3. Previous works comparison

Comparisons with the related works in EEG ScZ detection are listed in Table 10. In this study, the proposed method receives 98.47 ± 1.47 % accuracy, 99.26 ± 1.07 % sensitivity, and 97.23 ± 3.76 % specificity results in the testing data. Compared with the previous related work, the proposed method can achieve satisfactory detection results using the public LMSU dataset. In addition, the biomarkers of abnormal connectivity in DMN regions, temporal lobe and posterior temporal lobe area in both hemispheres are confirmed in this research.

This EEG based ScZ detection study still has some limitations. Sliding window technique is not an advanced method to cluster the dynamic state of brain activity. In addition, it is difficult to use the statistical analysis of whole brain connectivity to achieve high precision localization of ScZ disease. To overcome these limitations, the dynamic modelling analysis and source model reconstruction research will be the focus in our future research plan.

Table 7
EEG electrodes in the Brodmann areas of DMN regions [32].

DMN region	Brodmann area	EEG channel
LPC	BA39/40, Right	P4
LPC	BA39/40, Left	P3
MPC	BA08/09, Middle	Cz
MPC	BA08/09, Right	F4
MPC	BA08/09, Left	F3
PCC	BA07, Middle	Pz

TABLE 8
The mean value of connectivity values.

Abnormal connectivity	Connectivity values of ScZ	Connectivity values of HC
T4 - T6	0.496 ± 0.188	0.732 ± 0.134
F3 - F4	0.287 ± 0.136	0.441 ± 0.156
T3 - T5	0.558 ± 0.180	0.710 ± 0.147
Cz - P4	0.421 ± 0.125	0.538 ± 0.169
P4 - Pz	0.502 ± 0.137	0.609 ± 0.164
Cz - Pz	0.548 ± 0.134	0.651 ± 0.167

TABLE 9
Dynamic analysis of functional brain network.

Sliding window size	Accuracy (%)	Sensitivity (%)	Specificity (%)
3-second	87.91 ± 7.05	83.56 ± 6.99	90.00 ± 9.53
5-second	89.11 ± 5.59	85.30 ± 5.13	90.66 ± 9.01
10-second	90.20 ± 5.55	86.40 ± 5.78	92.10 ± 7.91
30-second	**98.47 ± 1.47**	**99.26 ± 1.07**	**97.23 ± 3.76**
40-second	90.89 ± 7.12	86.25 ± 8.62	94.56 ± 7.47

TABLE 10
Comparison of the related works in EEG ScZ detection.

Related works	Method	Accuracy (%)	Sensitivity (%)	Specificity (%)
Baygin, M et al (2021) [15]	Collatz pattern technique + k-NN	99.47	99.20	99.80
Akbari, H et al. (2021) [16]	Phase space dynamic features + k-NN	94.80	94.30	95.20
Lillo, E et al. (2022) [17]	CNN	93.00	–	–
Supakar, R et al. (2022) [18]	RNN - LSTM	98.00	98.00	98.00
Sairamya, N.J et al, (2022) [19]	DWT + RLNDip	100	–	–
Hassan, F et al. (2023) [20]	CNN + logistic regression	98.05 ± 1.13	99.00 ± 1.00	97.00 ± 2.00
Gosala, B et al. (2023) [21]	WST + SVM	97.98	98.20	97.72
Our previous work [24]	CMI + 3D-CNN	97.74 ± 1.15	96.91 ± 2.76	98.53 ± 1.97
Proposed method	MVAR coherence + 3D-CNN	98.47 ± 1.47	99.26 ± 1.07	97.23 ± 3.76

5. Conclusion

In contrast to existing research, this study distinguishes itself by furnishing invaluable biomarkers for ScZ and provides a high-accuracy detection approach of ScZ diseases. A new method proposed which includes the magnitude squared coherence algorithm and the MVAR model with a 1 Hz frequency resolution, coupled with the utilization of

the sliding window technique to capture dynamic brain connectivity. The magnitude squared coherence algorithm emerges as a standout performer in EEG ScZ detection, obtaining impressive metrics of 98.47 % accuracy, 99.26 % sensitivity, and 97.23 % specificity during evaluation and testing. In addition, the research identifies an optimal frequency band (8–12 Hz) for EEG ScZ detection, not only economizing computational resources but also shedding light on the connection between ScZ and disruptions in sensory gating and attention processes. Most critically, this study's findings illuminate the presence of irregular connectivity patterns in the DMN region, the temporal lobe, and the posterior temporal lobe, spanning both hemispheres of ScZ patients, thereby serving as promising biomarkers not only for the identification but also for the comprehension of neural anomalies associated with ScZ. The findings not only enrich the realm of ScZ research but also harbour significant potential for tangible clinical applications in the domain of ScZ detection and diagnosis.

Declaration of competing interest

The authors declare that they have no known competing financial interests or personal relationships that could have appeared to influence the work reported in this paper.

Data availability

No data was used for the research described in the article.

References

[1] J.N. Samsom, A.H. Wong, Schizophrenia and depression co-morbidity: what we have learned from animal models, Front. Psych. 6 (2015) 13.
[2] P.T. Krishnan, et al., Schizophrenia detection using multivariate empirical mode decomposition and entropy measures from multichannel EEG signal, Biocybernet. Biomed. Eng. 40 (3) (2020) 1124–1139.
[3] P. Krukow, et al., Abnormalities in hubs location and nodes centrality predict cognitive slowing and increased performance variability in first-episode schizophrenia patients, Sci. Rep. 9 (1) (2019) 9594.
[4] W. Pacific, S.A.W. Hasan, *Magnitude and impact.*.
[5] A. Craik, Y. He, J.L. Contreras-Vidal, Deep learning for electroencephalogram (EEG) classification tasks: a review, J. Neural Eng. 16 (3) (2019), 031001.
[6] G.G. Brown, W.K. Thompson, Functional brain imaging in schizophrenia: selected results and methods, Behav. Neurobiol. Schizophrenia Treatment (2010) 181–214.
[7] M.-h.R. Ho, et al., Time–frequency discriminant analysis of MEG signals, NeuroImage 40 (1) (2008) 174–186.
[8] Q. Long, et al., Independent vector analysis for common subspace analysis: application to multi-subject fMRI data yields meaningful subgroups of schizophrenia, Neuroimage 216 (2020), 116872.
[9] Z. Fu, et al., Dynamic state with covarying brain activity-connectivity: on the pathophysiology of schizophrenia, Neuroimage 224 (2021), 117385.
[10] G. Zhang, et al., Detecting abnormal connectivity in schizophrenia via a joint directed acyclic graph estimation model, Neuroimage 260 (2022), 119451.
[11] M.E. Raichle, et al., A default mode of brain function, Proc. Natl. Acad. Sci. 98 (2) (2001) 676–682.
[12] S. Zhang, et al., Abnormal default-mode network homogeneity and its correlations with neurocognitive deficits in drug-naive first-episode adolescent-onset schizophrenia, Schizophr. Res. 215 (2020) 140–147.
[13] J. Fan, et al., Resting-state default mode network related functional connectivity is associated with sustained attention deficits in schizophrenia and obsessive-compulsive disorder, Front. Behav. Neurosci. 12 (2018) 319.
[14] C.-R. Phang, et al., A multi-domain connectome convolutional neural network for identifying schizophrenia from EEG connectivity patterns, IEEE J. Biomed. Health Inform. 24 (5) (2019) 1333–1343.
[15] M. Baygin, et al., Automated accurate schizophrenia detection system using Collatz pattern technique with EEG signals, Biomed. Signal Process. Control 70 (2021), 102936.
[16] H. Akbari, et al., Schizophrenia recognition based on the phase space dynamic of EEG signals and graphical features, Biomed. Signal Process. Control 69 (2021), 102917.
[17] E. Lillo, M. Mora, B. Lucero, Automated diagnosis of schizophrenia using EEG microstates and Deep Convolutional Neural Network, Expert Syst. Appl. 209 (2022), 118236.
[18] R. Supakar, P. Satvaya, P. Chakrabarti, A deep learning based model using RNN-LSTM for the Detection of Schizophrenia from EEG data, Comput. Biol. Med. 151 (2022), 106225.
[19] N. Sairamya, M. Subathra, S.T. George, Automatic identification of schizophrenia using EEG signals based on discrete wavelet transform and RLNDiP technique with ANN, Expert Syst. Appl. 192 (2022), 116230.
[20] F. Hassan, S.F. Hussain, S.M. Qaisar, Fusion of multivariate EEG signals for schizophrenia detection using CNN and machine learning techniques, Information Fusion 92 (2023) 466–478.
[21] B. Gosala, et al., Wavelet transforms for feature engineering in EEG data processing: an application on Schizophrenia, Biomed. Signal Process. Control 85 (2023), 104811.
[22] J. Wang, et al., Discrimination of auditory verbal hallucination in schizophrenia based on EEG brain networks, Psychiatry Res. Neuroimaging 331 (2023), 111632.
[23] M. Prieto-Alcántara, et al., Alpha and gamma EEG coherence during on-task and mind wandering states in schizophrenia, Clin. Neurophysiol. 146 (2023) 21–29.
[24] M. Shen, et al., Automatic identification of schizophrenia based on EEG signals using dynamic functional connectivity analysis and 3D convolutional neural network, Comput. Biol. Med. (2023), 107022.
[25] N. Gorbachevskaya, S. Borisov, EEG data of healthy adolescents and adolescents with symptoms of schizophrenia, 2002.
[26] S. Borisov, et al., Analysis of EEG structural synchrony in adolescents with schizophrenic disorders, Hum. Physiol. 31 (3) (2005) 255–261.
[27] J.M. Seppänen, et al. Analysis of electromechanical modes using multichannel Yule-Walker estimation of a multivariate autoregressive model, in: IEEE PES ISGT Europe 2013, 2013, IEEE.
[28] G. Ippolito, et al., The role of alpha oscillations among the main neuropsychiatric disorders in the adult and developing human brain: evidence from the last 10 years of research, Biomedicines 10 (12) (2022) 3189.
[29] B.A. Seitzman, et al., The state of resting state networks, Topics in Magnetic Resonance Imaging: TMRI 28 (4) (2019) 189.
[30] D.A. Kaiser, Cortical cartography, Biofeedback 38 (1) (2010) 9–12.
[31] L. Koessler, et al., Automated cortical projection of EEG sensors: anatomical correlation via the international 10–10 system, Neuroimage 46 (1) (2009) 64–72.
[32] D.M. Khan, et al., Effective connectivity in default mode network for alcoholism diagnosis, IEEE Trans. Neural Syst. Rehabil. Eng. 29 (2021) 796–808.